

Noninvasive *in vivo* imaging of pancreatic islet cell biology

Stephan Speier^{1,5}, Daniel Nyqvist^{1,4,5}, Over Cabrera², Jia Yu¹, R Damaris Molano², Antonello Pileggi², Tilo Moede¹, Martin Köhler¹, Johannes Wilbertz³, Barbara Leibiger¹, Camillo Ricordi², Ingo B Leibiger¹, Alejandro Caicedo² & Per-Olof Berggren^{1,2}

Advanced imaging techniques have become a valuable tool in the study of complex biological processes at the cellular level in biomedical research. Here, we introduce a new technical platform for noninvasive *in vivo* fluorescence imaging of pancreatic islets using the anterior chamber of the eye as a natural body window. Islets transplanted into the mouse eye engrafted on the iris, became vascularized, retained cellular composition, responded to stimulation and reverted diabetes. Laser-scanning microscopy allowed repetitive *in vivo* imaging of islet vascularization, beta cell function and death at cellular resolution. Our results thus establish the basis for noninvasive *in vivo* investigations of complex cellular processes, like beta cell stimulus-response coupling, which can be performed longitudinally under both physiological and pathological conditions.

Adequate release of insulin by pancreatic beta cells in response to changing blood glucose levels is a vital requirement for maintaining glucose homeostasis. Failure to do so is one of the major causes of type 2 diabetes mellitus, the most common metabolic disorder in humans¹. Under physiological conditions, insulin release is regulated by the complex interplay between glucose and a plethora of additional factors—for example, nutrients, autocrine-paracrine signaling and the continuous input from hormones and neurotransmitters². Beta cells, together with other pancreatic endocrine cell types, are situated within the endocrine pancreas, that is, the islets of Langerhans, which are densely vascularized³ and abundantly innervated⁴. Pancreatic islets, constituting 1%–2% of the pancreatic volume, are difficult to access for *in vivo* monitoring because they are deeply embedded and scattered in the exocrine tissue of the pancreas⁵. As a consequence, the majority of functional beta cell studies have so far been conducted *in vitro* on isolated islets or beta cells. Isolated islets⁶, and especially pancreatic slices⁷, allow functional studies of beta cells in a multicellular environment. However, these studies are restricted to defined end-points, and the preparations partially lack input from vascular and nervous systems. Therefore, to fully understand the complexity of

beta cell signal transduction and the mechanisms controlling insulin release in health and disease, functional studies need to be conducted in vascularized and innervated islets *in vivo*. This concerns investigations not only of beta cell failure in type 2 diabetes, but also of islet function after transplantation, especially because clinical transplantation is emerging as a therapy for type 1 diabetes⁸. To date, monitoring beta cell signal transduction after islet transplantation has not been possible, and this has severely hampered both the characterization of graft function and the evaluation of new interventions⁹.

Laser-scanning microscopy (LSM) of isolated islets and cell preparations has been successfully applied for imaging multiple signaling pathways in the beta cell⁶. However, intravital applications of LSM for studies of beta cell physiology have not been reported. After transplantation, islets recruit a new vasculature¹⁰ and nervous connections¹¹ and are capable of maintaining glucose homeostasis via pulsatile insulin release^{11,12}, suggesting a re-established physiological environment. Our novel approach was to noninvasively image pancreatic islets, transplanted and engrafted in the anterior chamber of the eye, by using the cornea as a natural body window. The anterior chamber of the eye has been frequently used as a transplantation site to study a variety of tissues, including the pancreas^{13–15}, because it is an immune-privileged site and because the high amount of autonomic nerves and blood vessels found in the iris enables fast engraftment¹⁶.

RESULTS

The anterior chamber as a transplantation site for islets

Mouse islets were transplanted into the anterior chamber of the eye via injection through the cornea (**Fig. 1a**). After transplantation, islets engrafted on the iris and were readily observed and imaged through the cornea (**Fig. 1b,c**). The transplanted islets engrafted either as single islets or in groups as islet clusters (**Fig. 1c**). Islets that connected by a small surface area to the iris remained round. Other islet grafts attached to the iris by a large surface area and slightly flattened out. However, neither the degree of contact between islets and iris nor the form of the graft seemed to influence engraftment or function. Immunohistochemical staining of engrafted islets showed

¹The Rolf Luft Research Center for Diabetes and Endocrinology, Karolinska Institutet, Karolinska University Hospital L1, SE-17176 Stockholm, Sweden. ²Diabetes Research Institute, Miller School of Medicine, University of Miami, Northwest Tenth Avenue, Miami, Florida 33136, USA. ³Department of Cellular and Molecular Biology, Karolinska Institutet, von Eulers väg 3, SE-17177 Stockholm, Sweden. ⁴Current address: FIRI Institute of Molecular Oncology, Via Adamello 16, 20139 Milan, Italy. ⁵These authors contributed equally to this work. Correspondence should be addressed to P.O.B. (Per-Olof.Berggren@ki.se) or A.C. (acaicedo@med.miami.edu).

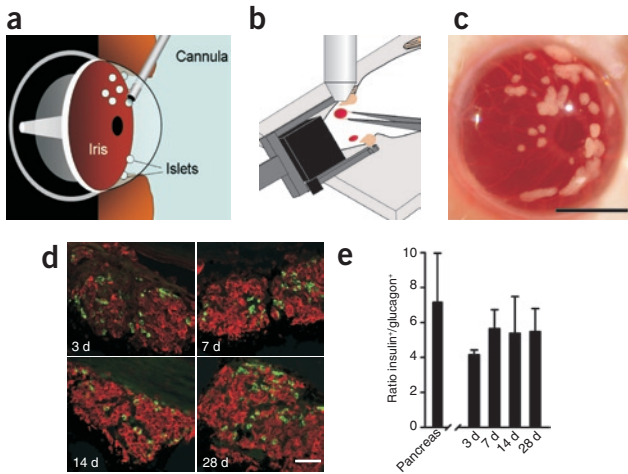


Figure 1 Pancreatic islet transplantation into the anterior chamber of the eye. **(a,b)** Illustration of islet transplantation into the anterior chamber of the eye and noninvasive *in vivo* imaging. **(c)** Photograph of islets engrafted on the iris. Scale bar, 2 mm. **(d)** Islet graft sections stained for insulin (red) and glucagon (green) at indicated time points after transplantation. Scale bar, 50 μ m. **(e)** Ratio of insulin⁺ to glucagon⁺ cells in islets in the pancreas and in the anterior chamber of the eye at the indicated time points after transplantation (differences are not significant; ANOVA, $P = 0.38$, $n = 4$ sections per pancreas, $n = 3-4$ mice per time point).

that the proportion of insulin-containing beta cells and glucagon-containing alpha cells did not change after transplantation and that this proportion was similar to that of islets in the pancreas (Fig. 1d,e), which is in agreement with earlier studies^{13,16}.

Noninvasive imaging of pancreatic islet vascularization

To allow identification of beta cells, islets isolated from transgenic mice expressing enhanced GFP under control of the rat insulin-1 promoter (RIP-GFP) were used for transplantation. Simultaneous two-photon LSM (TPLSM) of beta cells (GFP signal) and the vas-

cular network (intravenous Texas Red-conjugated 70-kDa dextran, revealed that transplanted islets recruit blood vessels from the iris. Noninvasive TPLSM enabled us to capture optical sections at different depths in the engrafted islets (Supplementary Fig. 1a-c online) and thereby reconstruct in three dimensions both beta cells and vascular morphology within the islet grafts (Supplementary Fig. 1d-f and Supplementary Video 1 online). We monitored the dynamics of islet engraftment and vascularization by imaging the same RIP-GFP islets at days 3, 7, 14 and 28, as well as 2 and 4 months after transplantation (Fig. 2a). At day 3, we observed transplanted islets attached to the iris and structural rearrangements of iris vessels in the vicinity of the islets. However, only a few vessels had grown into the peripheral regions of the islets. At day 7, islets showed an increased number of blood vessels, and capillary loops started to penetrate the central islet regions. After day 7, blood vessels continued to grow and, at day 14, formed a microvascular network throughout the islet grafts. Between day 14 and day 28, the vascular network became denser and, at day 28, was characterized by highly tortuous and uniformly sized capillaries. Imaging of islet grafts at 2 and 4 months after transplantation showed that the graft vascular network was similar to that at day 28. The vessel density continuously increased during revascularization up to day 28, when it finally reached a plateau (Fig. 2b). The diameter of islet graft vessels decreased after days 3 and 7, but remained unchanged after day 14. At day 28, the diameter was $8.11 \pm 0.53 \mu$ m ($n = 5$, Fig. 2c), which is similar to the intra-islet vasculature in the pancreas³ and other transplantation sites¹⁷.

Pancreatic islets engrafted in the eye maintain glucose homeostasis

We evaluated the overall function of engrafted islets by transplanting 300 islets into the anterior chamber of the eye of mice that were rendered diabetic before transplantation by streptozotocin treatment¹⁸. All mice became normoglycemic within 2 weeks (9.2 ± 2.2 d, $n = 4$) after transplantation and remained nondiabetic for over 200 d (Fig. 3a). These mice showed physiological responses to intraperitoneal glucose tolerance tests (6 weeks after transplantation) similar to those of healthy control mice (Fig. 3b). Nontransplanted, streptozotocin-treated mice were hyperglycemic at fasting and in response to glucose challenge (Fig. 3b). Removal of the graft-bearing eye resulted in prompt return to hyperglycemia (Fig. 3a), thus providing evidence that the glucose homeostasis had been controlled by the islets engrafted in the anterior chamber of the eye.

In vivo imaging of beta cell cytoplasmic free Ca²⁺ concentration

The ability to assess cell function *in vivo* at the cellular level would allow investigations of islet cell signal transduction mechanisms under physiological and pathological conditions, including regulatory and modulatory influences from paracrine, hormonal and neuronal signals. To monitor cell function *in vivo*, we studied changes in cytoplasmic free Ca²⁺ concentration ($[Ca^{2+}]_i$) of islets in the anterior chamber of the eye at the single-cell level. Changes in $[Ca^{2+}]_i$ are key intracellular signals in islet cells and serve as a reporter of beta cell function². Islets were loaded with the

© 2008 Nature Publishing Group <http://www.nature.com/naturemedicine>

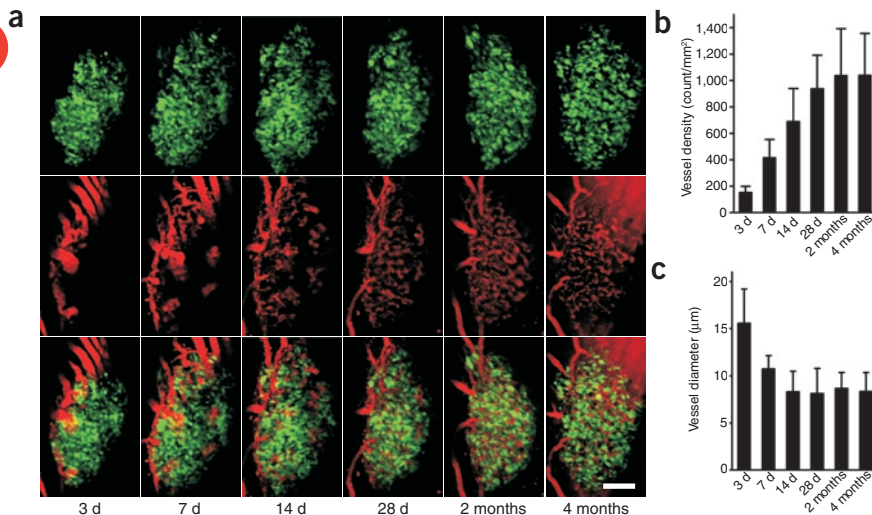


Figure 2 Noninvasive imaging of RIP-GFP islet engraftment and vascularization. **(a)** Maximum projections of image stacks (110- μ m thick) of an islet graft in the anterior chamber of the eye captured at indicated time points after transplantation. Top row, GFP fluorescence (beta cells); middle row, Texas Red fluorescence (blood vessels); bottom row, overlay of GFP and Texas Red. Two-photon excitation, 890 nm; objective: 10 \times 0.3 W; zoom factor, 2-2.3. Scale bar, 100 μ m. **(b,c)** Quantification of vessel density **(b)** and vessel diameter **(c)** in islet grafts at the indicated time points after transplantation ($n = 5$ for each time point).

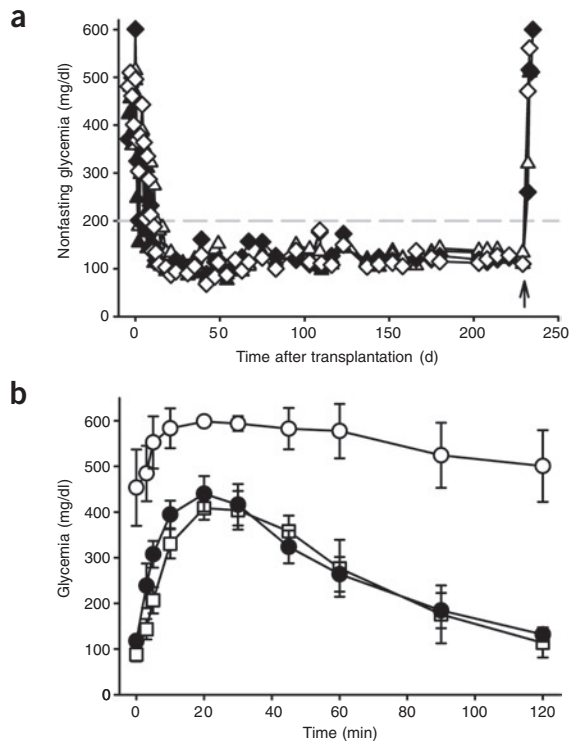


Figure 3 Pancreatic islets engrafted in the anterior chamber of the eye maintain glucose homeostasis. **(a)** Nonfasting glycemia in streptozotocin-induced diabetic mice after transplantation of islets (~300 islet equivalents) to the anterior chamber of the eye ($n = 4$; \blacktriangle , \diamond , \blacklozenge and \triangle each correspond to one mouse). Removal of the islet graft-bearing eye is indicated by the arrow. Dashed line indicates upper limit for normoglycemia. **(b)** Plasma glucose levels during intraperitoneal glucose tolerance tests performed 6 weeks after transplantation of islets in the anterior chamber of the eye (\square , $n = 4$), in normal controls (\bullet , $n = 9$), and in streptozotocin-induced diabetic mice (\circ , $n = 7$).

cell activity, because in similar experiments, alpha cells, although loaded with the Ca^{2+} indicator and situated in the outer cell layer of the islet, do not respond with an increase in $[\text{Ca}^{2+}]_i$ to stimulation with glibenclamide²⁰. $[\text{Ca}^{2+}]_i$ increased simultaneously in different regions of the islets, reflecting the synchronized response of beta cells within an islet to stimulation²¹ (**Fig. 4c,d**). To record changes in $[\text{Ca}^{2+}]_i$ from the same islet cells repeatedly, we perfused the anterior chamber with Fluo-4 and Fura-Red at different days. Increases in the Fluo-4/Fura-Red ratio were measured from the same islet in response to stimulation (**Fig. 4e**).

Noninvasive *in vivo* imaging of beta cell death

Beta cell death is the cause of type 1 diabetes²² and is implicated in the pathology of type 2 diabetes²³. To date, no methods exist for continuous monitoring of beta cell death *in vivo*. Annexin V has been used as a reporter of cell death under experimental and clinical conditions²⁴ and has been validated as a marker for beta cell death after systemic administration²⁵. To investigate the possibility of non-invasive imaging of beta cell death, we transplanted RIP-GFP islets into the anterior chamber of the eye and, after complete engraftment and vascularization, monitored cell death after intravenous administration of annexin V conjugated to allophycocyanin (APC). Using confocal LSM, we captured GFP and annexin V-APC fluorescence simultaneously, together with reflected light, which provided structural information about the endocrine cells²⁶ (**Fig. 5**). Transplanted RIP-GFP islets imaged in mice with regular blood glucose levels showed normal morphology (**Fig. 5a,c**) and an absence of annexin V-APC labeling (**Fig. 5b,d**). Annexin V-APC was only found to label a few cells in one out of ten RIP-GFP islet grafts (data not shown), indicating a low incidence of cell death in islets engrafted in the

Ca^{2+} indicators Fluo-4 and Fura-Red via perfusion of the anterior chamber of the eye (**Fig. 4**). Applying these two dyes simultaneously allowed for ratiometric measurements of $[\text{Ca}^{2+}]_i$ changes with LSM and correction for movements of the islets during imaging¹⁹. Fluo-4 and Fura-Red labeled the outer layer of the islets homogeneously (**Fig. 4a,d** and **Supplementary Video 2** online). To stimulate beta cells, the sulfonylurea compound glibenclamide was applied intravenously. This led to a decrease in blood glucose as a result of insulin release, indicating that the administration was effective (data not shown). Increases in $[\text{Ca}^{2+}]_i$ in beta cells in the islet grafts, as indicated by prominent rises in the Fluo-4/Fura-Red fluorescence ratio, started within 30–40 s after injection of glibenclamide into the tail vein and remained high throughout the recording (**Fig. 4b** and **Supplementary Video 3** online). These responses indicated beta

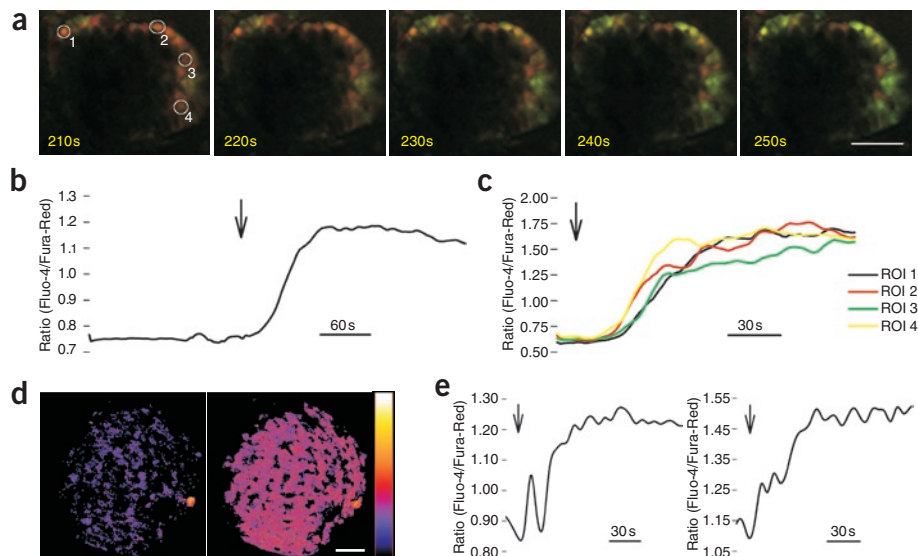


Figure 4 Noninvasive *in vivo* imaging of beta cell $[\text{Ca}^{2+}]_i$ handling. **(a)** Fluorescence images of Fluo-4 and Fura-Red at indicated time points after systemic application of glibenclamide (1 mg/kg) at 180 s, 3 months after transplantation. Excitation, 488 nm; objective, $20\times$ W 0.5; zoom factor, 2.3; pinhole, 1 airy unit. **(b)** Whole-frame Fluo-4/Fura-Red ratio change in response to glibenclamide stimulus (arrow indicates stimulation start). **(c)** Ratio change in individual cells within the imaging plane as indicated in panel **a**. ROI, region of interest. **(d)** Ratiometric maximum projections of Fluo-4/Fura-Red of a whole islet before (left) and after (right) glibenclamide stimulation. Excitation, 488 nm; objective, $20\times$ W 0.5; zoom factor, 1.7, pinhole, 1 airy unit. **(e)** A representative Fluo-4/Fura-Red ratio change in response to a glibenclamide stimulus, start as indicated by arrows, recorded from the same islet graft at days 34 (left) and 37 (right) after transplantation. Scale bars, 50 μm .

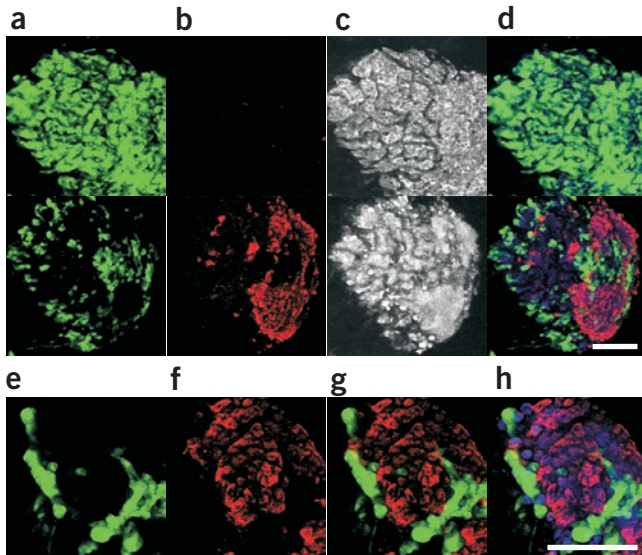


Figure 5 Noninvasive *in vivo* imaging of beta cell death. (a–h) Maximum projections of image stacks (260- μ m thick) captured of an individual RIP-GFP islet graft in the anterior chamber of the eye 2 months after transplantation. Excitation, 488, 543 and 633 nm; objective, 20 \times W 0.5 (a–d) and 40 \times W 0.8 (e–h); zoom factor, 1.7; pinhole: 1 airy unit. (a–d) GFP fluorescence (beta cells, a), annexin V-APC labeling (b), reflected light of the islet graft (c) and overlay of a–c (d) with reflected light in blue under normoglycemic conditions (top row) and under hyperglycemic conditions 24 h after alloxan treatment (bottom row). (e–h) High magnification images of a RIP-GFP islet graft area strongly labeled with annexin V-APC after alloxan-induced beta cell death. (e) GFP fluorescence (beta cells). (f) Annexin V-APC fluorescence. (g) Overlay of e and f. (h) Overlay of g and reflected light in blue. Scale bars, 100 μ m.

anterior chamber of the eye. Beta cell death in mice transplanted with RIP-GFP islets was induced by intravenous administration of alloxan (75 mg/kg)¹⁸. This treatment rendered mice hyperglycemic, with a blood glucose concentration of 450.0 ± 23.4 mg/dl ($n = 6$) after 24 h. At this time point, substantial loss of GFP fluorescence and structural changes in the reflection of the islet grafts were observed (Fig. 5a,c), indicating a loss of beta cells. Administration of annexin V-APC ($n = 4$) 24 h after the induction of cell death resulted in strong labeling of islet grafts (Fig. 5b,d). High-magnification imaging revealed that most annexin V-APC labeling was in graft regions devoid of GFP fluorescence (Fig. 5e–h). This observation is in agreement with previous reports describing rapid loss of GFP fluorescence in cells after induction of apoptosis or necrosis²⁷. Some annexin V-APC fluorescence was found on the surface of GFP-fluorescent beta cells, indicating cells in the early stages of the apoptotic process.

DISCUSSION

We have introduced a new platform for noninvasive and longitudinal studies of pancreatic islet cell biology *in vivo*. Transplantation of isolated islets to the anterior chamber of the eye is minimally invasive compared to transplantation procedures to other sites and is followed by a short recovery period, thus limiting both surgical and post-transplantation stress. Imaging of islets engrafted in the anterior chamber of the eye through the cornea is noninvasive and therefore considerably reduces the manipulations needed to access the target tissue *in vivo*.

After transplantation, the morphology and cellular composition of the islets engrafting in the anterior chamber of the eye are preserved. Furthermore, the engrafted islets participate in blood glu-

cose control and are able to maintain glucose homeostasis in the absence of endogenous pancreatic beta cells. By using the anterior chamber of the eye as an *in vivo* model for islet cell research, we were able to longitudinally monitor the vascular network, as well as signal transduction processes involved in beta cell function and death. In the future, this will enable *in vivo* studies measuring not only graft vascularization and its modulation by physiological and pathological factors, but also the interaction between endothelial and endocrine cells within the islet²⁸. Furthermore, the use of this platform to study islet cell function and survival *in vivo* will help to clarify the effects of modulatory inputs by hormonal and neuronal systems, as well as autocrine and paracrine signals of endocrine or vascular cells. It will also serve as a unique approach for noninvasive *in vivo* studies of beta cell function and survival under both physiological and diabetic conditions. Finally, we are convinced that this *in vivo* experimental model system in the anterior chamber of the eye can also be applied in investigations of endocrine pancreas development and drug screening. It is noteworthy that this platform is not limited to studies of cells of the endocrine pancreas, but can readily be extended to investigations of numerous other cell types and organ tissues *in vivo*. Hence, the anterior chamber of the eye, as a natural body window, can be used as a versatile tool to clarify the integration of complex signaling networks at the cellular level under *in vivo* conditions.

METHODS

Mouse models. We purchased C57BL6, NMRI and Tie2-GFP mice (STOCK Tg(TIE2GFP)287Sato/J) from the Jackson Laboratories. We generated RIP-GFP mice at a core facility at Karolinska Institutet, and they show a normal glucose tolerance (see **Supplementary Methods** online). All experiments were approved by the local animal ethics committees at Karolinska Institutet (Local Animal Ethics Committee of Karolinska Institutet) and the University of Miami (University of Miami Animal Care and Use Committee).

Transplantation of pancreatic islets to the anterior chamber of the eye. We isolated and cultured pancreatic islets as previously described^{26,29}. For transplantation, we transferred 30–300 islets from culture media to sterile PBS and aspirated them into a blunt 27-gauge eye cannula connected to a 1-ml Hamilton syringe (Hamilton) via 0.4-mm polythene tubing (Portex Limited). We anesthetized mice using isoflurane (Abott Scandinavia) or a mix of ketamine (80–100 mg/kg; Fort Dodge) and xylazine (5–10 mg/kg; Phoenix Pharmaceutical). To obtain post-operative analgesia, we applied Temgesic (0.1 ml/kg; Schering-Plough) or butrenorphine (0.05 mg/kg; Reckitt Benckiser Pharmaceuticals). Under a stereomicroscope, we punctured the cornea close to the sclera at the bottom part of the eye with a 27-gauge needle and took great care not to damage the iris and to avoid bleeding. Next, we gently inserted the blunt eye cannula and slowly injected the islets into the anterior chamber, where they settled onto the iris. After injection, we carefully withdrew the cannula and left the mouse lying on its side before awakening. The mice quickly recovered and showed no signs of stress or irritation from the manipulated eye.

***In vivo* imaging of islets transplanted to the anterior chamber of the eye.** At the indicated time points after transplantation (see Results and figure legends), we anesthetized mice with a 40% oxygen and a ~2.5% isoflurane mixture and placed them on a heating pad. We restrained the mouse head with a stereotaxic headholder (SG-4N, Narishige) and positioned the eye containing the engrafted islets facing upwards. We carefully pulled back the eyelid and held the eye gently at the corneoscleral junction with a pair of tweezers attached to a UST-2 Solid Universal Joint (Narishige). The tips of the tweezers were covered with a single piece of polythene tubing, creating a loop between the two tips. This arrangement permitted a flexible but stable fixation of the head and eye without causing damage or disrupting the blood circulation in the eye. For imaging, we used an upright Leica DMLFSA microscope equipped with a TCS-SP2-AOBS confocal scanner (Leica Microsystems) and lasers for two-photon excitation²⁶, together with long-distance water-dipping lenses (Leica HXC APO 10 \times 0.3W, 20 \times 0.5 W, 40 \times 0.8W).

As immersion liquid, we used filtered saline or Viscotears (Novartis). We performed confocal LSM and TPLSM imaging employing the minimum required laser-power and scan-time necessary. We observed no signs of photo-damage in islet cells or blood vessels during the work with this experimental model. To de-noise the images captured with confocal LSM and TPLSM, we used wavelet filtering as previously described³⁰, and for display purposes we applied contrast enhancement to the images. We used Leica Confocal Software (version 2.61), Volocity (Improvision) and ImageJ to process images. For visualization of blood vessels, we intravenously injected Texas Red (100 µl of 10 mg/ml; Molecular Probes) via the tail vein. We excited GFP and Texas Red at 890 nm and separated and collected emission light onto two nondescanned detectors using a dichroic mirror (RSP560) and emission filters (BP 525/50 and BP 640/20). For visualization of cell death, we intravenously injected 100 µl of annexin V-APC (Molecular Probes) via the tail vein. We excited GFP at 488 nm and collected emission light between 495 nm and 530 nm. To image reflected light, we illuminated at 546 nm and collected between 539 nm and 547 nm. We excited APC at 633 nm with collection of emission light between 644 nm and 680 nm. Initial studies showed weak annexin V-APC labeling of RIP-GFP islet grafts ~40 min after administration with a gradual increase. We imaged the islet grafts 4–6 h after administration of annexin V-APC.

Statistical analyses. Data are presented as mean ± s.d. Significance was tested using an analysis of variance (ANOVA) and indicated in the figure legend.

Note: Supplementary information is available on the Nature Medicine website.

ACKNOWLEDGMENTS

This study was supported by grant DK-58508 and DK-075487 (to A.C.) from the US National Institutes of Health, Juvenile Diabetes Research Foundation International grant 3-2007-73 (to S.S.) and 4-2004-361, the Swedish Research Council, the Novo Nordisk Foundation, Karolinska Institutet, the Swedish Diabetes Association, The Family Knut and Alice Wallberg Foundation, Eurodia (FP6-518153), European Foundation for the Study of Diabetes, the European Foundation for the Study of Diabetes–Lilly Research Program, Berth von Kantzow's Foundation, the Family Erling-Persson Foundation and the Diabetes Research Institute Foundation.

AUTHOR CONTRIBUTIONS

S.S., D.N. and A.C. developed the experimental transplantation platform. S.S., D.N., O.C., J.Y., R.D.M., A.P., T.M., M.K., B.L. and A.C. did the experiments. J.W. was responsible for generating the transgenic mice. C.R. was involved in designing the transplantation protocols and writing the manuscript. S.S., D.N., I.B.L. and P.-O.B. were responsible for designing the overall experimental plan and writing the manuscript. P.-O.B. was the originator of the idea of using the anterior chamber of the eye for noninvasive *in vivo* imaging of pancreatic islet cell biology.

Published online at <http://www.nature.com/naturemedicine>

Reprints and permissions information is available online at <http://npg.nature.com/reprintsandpermissions>

1. Wajchenberg, B.L. Beta cell failure in diabetes and preservation by clinical treatment. *Endocr. Rev.* **28**, 187–218 (2007).
2. Berggren, P.O. & Leibiger, I.B. Novel aspects on signal transduction in the pancreatic beta cell. *Nutr. Metab. Cardiovasc. Dis. 16 Suppl 1*, S7–S10 (2006).
3. Vetterlein, F., Petho, A. & Schmidt, G. Morphometric investigation of the microvascular system of pancreatic exocrine and endocrine tissue in the rat. *Microvasc. Res.* **34**,

- 231–238 (1987).
4. Woods, S.C. & Porte, D., Jr. Neural control of the endocrine pancreas. *Physiol. Rev.* **54**, 596–619 (1974).
5. Rahier, J., Goebbels, R.M. & Henquin, J.C. Cellular composition of the human diabetic pancreas. *Diabetologia* **24**, 366–371 (1983).
6. Köhler, M. *et al.* Imaging of pancreatic beta cell signal transduction. *Curr. Med. Chem.-Immun. Endoc. & Metab. Agents* **4**, 281–299 (2004).
7. Speier, S. & Rupnik, M. A novel approach to *in situ* characterization of pancreatic beta cells. *Pflugers Arch.* **446**, 553–558 (2003).
8. Ricordi, C. Islet transplantation: a brave new world. *Diabetes* **52**, 1595–1603 (2003).
9. Paty, B.W., Bonner-Weir, S., Laughlin, M.R., McEwan, A.J. & Shapiro, A.M. Toward development of imaging modalities for islets after transplantation: insights from the National Institutes of Health Workshop on Beta Cell Imaging. *Transplantation* **77**, 1133–1137 (2004).
10. Menger, M.D., Yamauchi, J. & Vollmar, B. Revascularization and microcirculation of freely grafted islets of Langerhans. *World J. Surg.* **25**, 509–515 (2001).
11. Porksen, N. *et al.* Coordinate pulsatile insulin secretion by chronic intraportally transplanted islets in the isolated perfused rat liver. *J. Clin. Invest.* **94**, 219–227 (1994).
12. Meier, J.J. *et al.* Intrahepatic transplanted islets in humans secrete insulin in a coordinate pulsatile manner directly into the liver. *Diabetes* **55**, 2324–2332 (2006).
13. Adeghate, E. & Donath, T. Morphological findings in long-term pancreatic tissue transplants in the anterior eye chamber of rats. *Pancreas* **5**, 298–305 (1990).
14. Hoffer, B., Seiger, A., Ljungberg, T. & Olson, L. Electrophysiological and cytological studies of brain homografts in the anterior chamber of the eye: maturation of cerebellar cortex in oculo. *Brain Res.* **79**, 165–184 (1974).
15. Katoh, N. *et al.* Target-specific innervation by autonomic and sensory nerve fibers in hairy fetal skin transplanted into the anterior eye chamber of adult rat. *Cell Tissue Res.* **266**, 259–263 (1991).
16. Adeghate, E., Ponery, A.S., Ahmed, I. & Donath, T. Comparative morphology and biochemistry of pancreatic tissue fragments transplanted into the anterior eye chamber and subcutaneous regions of the rat. *Eur. J. Morphol.* **39**, 257–268 (2001).
17. Menger, M.D., Vajkoczy, P., Leiderer, R., Jager, S. & Messmer, K. Influence of experimental hyperglycemia on microvascular blood perfusion of pancreatic islet isografts. *J. Clin. Invest.* **90**, 1361–1369 (1992).
18. Szkudelski, T. The mechanism of alloxan and streptozotocin action in B cells of the rat pancreas. *Physiol. Res.* **50**, 537–546 (2001).
19. Lipp, P. & Niggli, E. Ratiometric confocal Ca²⁺ measurements with visible wavelength indicators in isolated cardiac myocytes. *Cell Calcium* **14**, 359–372 (1993).
20. Quesada, I., Nadal, A. & Soria, B. Different effects of tolbutamide and diazoxide in alpha, beta, and delta cells within intact islets of Langerhans. *Diabetes* **48**, 2390–2397 (1999).
21. Valdeolmillos, M., Santos, R.M., Contreras, D., Soria, B. & Rosario, L.M. Glucose-induced oscillations of intracellular Ca²⁺ concentration resembling bursting electrical activity in single mouse islets of Langerhans. *FEBS Lett.* **259**, 19–23 (1989).
22. Mathis, D., Vence, L. & Benoist, C. Beta cell death during progression to diabetes. *Nature* **414**, 792–798 (2001).
23. Butler, A.E. *et al.* Beta cell deficit and increased beta cell apoptosis in humans with type 2 diabetes. *Diabetes* **52**, 102–110 (2003).
24. Boersma, H.H. *et al.* Past, present, and future of annexin A5: from protein discovery to clinical applications. *J. Nucl. Med.* **46**, 2035–2050 (2005).
25. Medarova, Z., Bonner-Weir, S., Lipes, M. & Moore, A. Imaging beta cell death with a near-infrared probe. *Diabetes* **54**, 1780–1788 (2005).
26. Nyqvist, D., Köhler, M., Wahlstedt, H. & Berggren, P.O. Donor islet endothelial cells participate in formation of functional vessels within pancreatic islet grafts. *Diabetes* **54**, 2287–2293 (2005).
27. Strebler, A., Harr, T., Bachmann, F., Wernli, M. & Erb, P. Green fluorescent protein as a novel tool to measure apoptosis and necrosis. *Cytometry* **43**, 126–133 (2001).
28. Nikolova, G. *et al.* The vascular basement membrane: a niche for insulin gene expression and beta cell proliferation. *Dev. Cell* **10**, 397–405 (2006).
29. Berney, T. *et al.* Endotoxin-mediated delayed islet graft function is associated with increased intra-islet cytokine production and islet cell apoptosis. *Transplantation* **71**, 125–132 (2001).
30. Köhler, M. *et al.* On-line monitoring of apoptosis in insulin-secreting cells. *Diabetes* **52**, 2943–2950 (2003).